ACS chemical biology

ARTICLE

Phosphorylation and Processing of the Quorum-Sensing Molecule Autoinducer-2 in Enteric Bacteria

Karina B. Xavier[†,‡,§], Stephen T. Miller[¶], Wenyun Lu[∥], Jeong Hwan Kim[¶], Joshua Rabinowitz[∥], István Pelczer[**], Martin F. Semmelhack[**], and Bonnie L. Bassler[†,††,*]

[†]Department of Molecular Biology, Princeton University, Princeton, New Jersey 08544-1014, [‡]Instituto de Tecnologia Química e Biológica, Universidade Nova de Lisboa, Apt. 127, P-2780-156 Oeiras, Portugal, [§]Instituto Gulbenkian de Ciência, Apt. 14, P-2781-901 Oeiras, Portugal, [¶]Department of Chemistry and Biochemistry, Swarthmore College, Swarthmore, Pennsylvania 19081, [∥]Department of Chemistry and Lewis-Sigler Institute for Integrative Genomics, Princeton University, Princeton, New Jersey 08544-1014, [**]Department of Chemistry, Princeton University, Princeton, New Jersey 08544-1014, [††]Howard Hughes Medical Institute, 4000 Jones Bridge Road, Chevy Chase, Maryland 20815-6789

ABSTRACT Quorum sensing is a process of chemical communication that bacteria use to assess cell population density and synchronize behavior on a community-wide scale. Communication is mediated by signal molecules called autoinducers. The LuxS autoinducer synthase produces 4,5-dihydroxy-2,3-pentanedione (DPD), the precursor to a set of interconverting molecules that are generically called autoinducer-2 (AI-2). In enteric bacteria, AI-2 production induces the assembly of a transport apparatus (called the LuxS regulated (Lsr) transporter) that internalizes endogenously produced AI-2 as well as AI-2 produced by other bacterial species. AI-2 internalization is proposed to be a mechanism enteric bacteria employ to interfere with the signaling capabilities of neighboring species of bacteria. We have previously shown that *Salmonella enterica* serovar Typhimurium binds a specific cyclic derivative of DPD. Here we show that following internalization, the kinase LsrK phosphorylates carbon-5 of the open form of DPD. Phosphorylated DPD (P-DPD) binds specifically to the repressor of the *lsr* operon, LsrR, consistent with P-DPD being the inducer of the *lsr* operon. Subsequently, LsrG catalyzes the cleavage of P-DPD producing 2-phosphoglycolic acid. This series of chemical events is proposed to enable enteric bacteria to respond to the presence of competitor bacteria by sequestering and destroying AI-2, thereby eliminating the competitors' intercellular communication capabilities.

*Corresponding author,
bbassler@princeton.edu.

Received for review November 5, 2006
and accepted January 4, 2007.

Published online February 2, 2007

10.1021/cb600444h CCC: $37.00

Bacteria communicate with chemical signal molecules called autoinducers. This process, called quorum sensing, enables bacteria to count the members in the vicinal community and, in response to changes in population density, alter gene expression in unison (*1*). Production and detection of most autoinducers are restricted to organisms within a species. By contrast, the autoinducer generically called autoinducer-2 (AI-2), which is a family of interconverting molecules all derived from a common precursor, is produced and detected by a wide variety of bacteria. Thus, AI-2 has been termed a "universal" bacterial signal. Many bacteria control a variety of niche-specific behaviors in response to AI-2 (*2*–*4*); however, the mechanisms of AI-2 detection and signal transduction have only been determined in two *Vibrio* species and the enteric bacteria *Escherichia coli* and *Salmonella enterica* serovar Typhimurium (*5*–*9*).

In all AI-2-producing bacteria, the precursor for the AI-2 signal is 4,5-dihydroxy-2,3-pentanedione (DPD), the product of the reaction catalyzed by the LuxS enzyme ((*10, 11*) and Figure 1, panel a). DPD is a highly reactive molecule that rearranges and undergoes additional spontaneous reactions in solution. Distinct but related molecules are derived from DPD, and different bacterial species recognize various forms of DPD as AI-2 signals. To date, we have identified two different DPD-derived signals by trapping the active AI-2 signals in their respective AI-2 receptors (the LuxP protein from *Vibrio harveyi*, and the LsrB protein from the enteric bacterium *S. typhimurium*), crystallizing the complexes, and solving their structures (*5, 7*). In *V. harveyi*, the AI-2 signal is

formed by cyclization, hydration, and addition of borate to DPD. In enteric bacteria, the LsrB protein recognizes an AI-2 moiety that lacks boron and is a different stereoisomer than the signal recognized by *V. harveyi* (Figure 1, panel a). Importantly, these two molecules interconvert rapidly in solution (*7*). Because the AI-2s interconvert, bacteria that detect distinct DPD derivatives can nonetheless communicate with one another (*12*).

In *S. typhimurium* and *E. coli*, AI-2 controls the expression of a transporter (called LuxS regulated (Lsr)) responsible for internalizing, phosphorylating, and processing of the AI-2 signal (*8, 9, 13*). The Lsr transporter is encoded by the genes in the *lsr* operon, and their expression is activated by AI-2. In the absence of AI-2, LsrR represses the *lsr* operon (Figure 1, panel b). Following AI-2 release, low-level internalization occurs, and intracellular AI-2 is phosphorylated by the cytoplasmic LsrK kinase. Our genetic studies have shown that phosphorylation of the AI-2 signal leads to derepression of *lsr* expression, assembly of the Lsr transporter, and rapid AI-2 internalization. We suspect that a phosphorylated form of AI-2 binds and antagonizes LsrR, raising the possibility that this phosphorylated form of AI-2 is the intracellular signal responsible for *lsr* activation. The *lsrF* and *lsrG* genes, which are encoded in the *lsr* operon, are involved in the further processing of the internalized signal because expression of the *lsr* operon increases significantly in *lsrFG* double mutants (*13*). We have hypothesized that in the *lsrFG* mutant, increased *lsr* expression is a result of cytoplasmic accumulation of phosphorylated AI-2. Moreover, complementation tests revealed that overexpression of either *lsrF* or *lsrG* individually brings the expression of the *lsr* operon down to wild-type levels, suggesting that each of these genes is involved in processing of the internalized molecule. The LsrF protein has homology to sugar-phosphate aldolases, and LsrG does not have homology to proteins of known function.

Here we use thin layer chromatography (TLC), mass spectrometry (MS), and NMR with purified proteins and synthetically prepared DPD to identify the phosphorylated form of AI-2 and characterize the processing of the AI-2 signal in enteric bacteria. Our analysis of the LsrK reaction shows that LsrK phosphorylates the ring-open form of DPD at the C5 position, and that phosphorylated DPD (P-DPD) binds directly to the repressor LsrR. LsrG

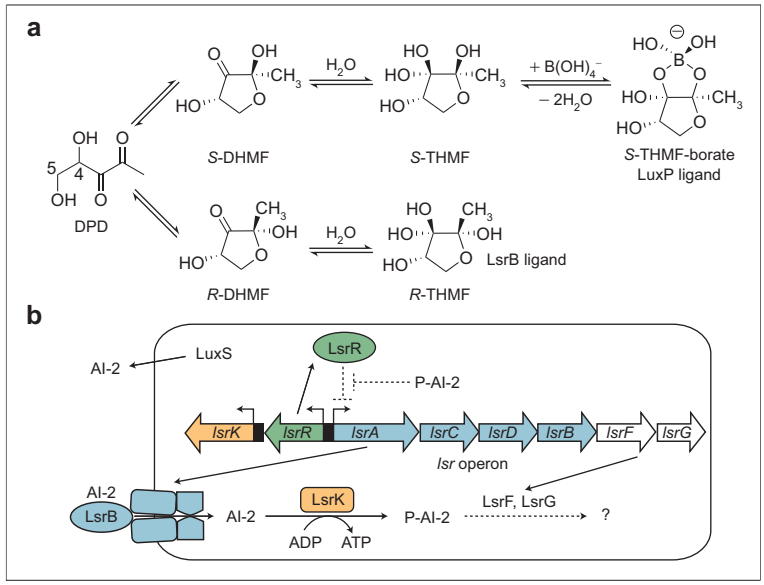

Figure 1. The AI-2 family of signaling molecules and Lsr-mediated transport and processing of AI-2. a) DPD is the product of the LuxS enzyme and the precursor to all AI-2 signaling molecules. In solution, DPD cyclizes spontaneously to form two epimeric furanoses, (2*R*,4*S*)- and (2*S*,4*S*)-2,4-dihydroxy-2-methyldihydrofuran-3-one (*R*- and *S*-DHMF, respectively). Hydration of *R*- and *S*-DHMF gives rise to *R*- and *S*-THMF, respectively. Two active AI-2 molecules were identified by trapping them in their respective binding proteins. This analysis revealed that the *V. harveyi* receptor, LuxP, detects a borated form of *S*-THMF (*S*-THMF-borate) and the *S. typhimurium* receptor, LsrB, detects *R*-THMF. b) In *S. typhimurium* and *E. coli*, AI-2 is produced by the reaction catalyzed by LuxS and is released into the extracellular environment. AI-2 is bound by the periplasmic protein LsrB and internalized by the Lsr ATP-binding cassette-type transporter, and intracellular AI-2 is phosphorylated by LsrK. A phosphorylated form of AI-2 (P-AI-2) induces *lsr* transcription and is proposed to act by binding to LsrR, the repressor of the *lsr* operon, thereby inactivating it. Induction of *lsr* expression causes rapid Lsr-dependent AI-2 internalization. The LsrF and LsrG proteins are also encoded by the *lsr* operon and are required for the further processing of intracellular P-AI-2. The *S. typhimurium lsr* operon contains an additional gene downstream of *lsrG*, called *lsrE*, which is not present in the *E. coli* operon. The *lsrE* gene is homologous to genes encoding sugar epimerases. Dotted lines represent hypothetical interactions.

subsequently cleaves P-DPD, producing 2-phosphoglycolic acid (PG). Degradation of P-DPD terminates induction of the *lsr* operon and, in turn, closes the AI-2 signaling cycle.

RESULTS AND DISCUSSION

LsrK Is a Kinase That Phosphorylates DPD. Previous studies established that LsrK is a kinase that phosphorylates synthetically prepared DPD with the simultaneous conversion of ATP to ADP (*13*). Our results (Figure 2, panel a) demonstrate this point; incubation of [γ-^{32}P]ATP with LsrK and DPD results in the disappear-

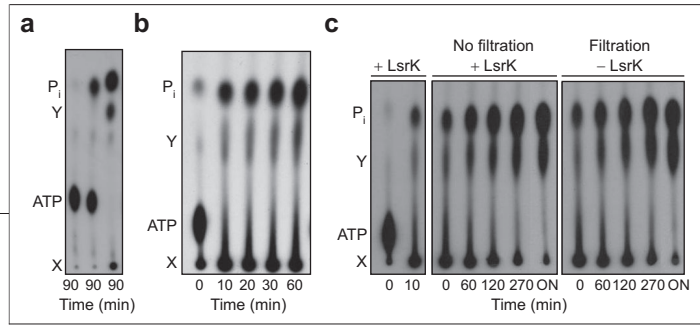

Figure 2. Analysis of the LsrK reaction. TLC plate with [γ-^{32}P]ATP, P_i, and the phosphorylated products (X and Y) marked. a) Lanes from left to right contained aliquots from reactions with [γ-^{32}P]ATP only; [γ-^{32}P]ATP and LsrK; and [γ-^{32}P]ATP, LsrK, and DPD. Aliquots were applied to the TLC plate after 90 min incubation. b) LsrK was incubated with [γ-^{32}P]ATP and DPD, and at the specified times, aliquots were removed from the reaction and applied to the TLC plate. c) The left-most TLC plate shows DPD and [γ-^{32}P]ATP following 0 and 10 min incubation with LsrK. The middle TLC plate shows the results following continued incubation. The right-most TLC plate shows the results following removal of the LsrK protein by filtration and then continued incubation. ON denotes overnight.

ance of ATP, the appearance of two radiolabeled products (denoted X and Y), and the production of radiolabeled inorganic phosphate (P_i). One of the new species (X) remains at the origin of the TLC plate, while the other (Y) migrates. The controls (first and second lanes) show that, in the absence of the DPD substrate, incubation of LsrK with [γ-^{32}P]ATP results in some low-level ATP hydrolysis. The two phosphorylated products are, however, formed only in the presence of all the components of the reaction (third lane).

Our finding that the reaction catalyzed by LsrK with DPD as the substrate yields two phosphorylated species was unexpected. Time-course analysis (Figure 2, panel b) of the reaction shows that only the immobile species X is the product of the LsrK-catalyzed reaction with DPD. Specifically, a brief 10 min incubation of LsrK, DPD, and ATP is sufficient for full consumption of ATP and formation of the phosphorylated, immobile product X. Small amounts of the second product Y are detected only after significantly longer incubation (60 min). Because product Y appeared to be formed only following production of X, we wondered whether Y was derived from X by an LsrK-independent (*i.e.*, spontaneous) mechanism. To test this idea, we ran the LsrK reaction for 10 min to produce X and only trace amounts of Y (Figure 2, panel c, left). We immediately subjected half of the reaction mixture to filtration to remove the LsrK enzyme. Subsequently, we monitored the mixtures containing and lacking LsrK for the products X and Y. Production of Y occurred at an identical rate irrespective of the presence or absence of the LsrK enzyme (Figure 2, panel c, middle and right). This result shows that product Y is made from product X *via* a mechanism that does not involve the LsrK enzyme. On the basis of this series of experiments, we suggest that X, the immediate product of LsrK reaction with DPD is P-DPD. This hypothesis is verified by several methods below.

The LsrR Repressor Binds P-DPD. Genetic analysis has shown that LsrR represses the *lsr* operon, and following LsrK action on internalized DPD, LsrR repression of the *lsr* operon is relieved (*9, 13*, and Figure 1, panel b). LsrK phosphorylates DPD (Figure 2), consistent with P-DPD being the moiety required for inactivation of LsrR. We hypothesized that LsrR binding to P-DPD could be the event that inactivates LsrR as a repressor, leading to induction of *lsr* operon expression. To test this possibility, we purified the LsrR protein and incubated it for 10 min with the products of reaction of LsrK with DPD and [γ-^{32}P]ATP (Figure 3, lane 1). We filtered the sample and subjected the filtrate to TLC analysis. We also washed the LsrR protein fraction extensively and spotted the washed protein onto the TLC plate. Both phosphorylated products X and Y can be detected in the protein-free filtrate (Figure 3, lane 2). However, only product X is detected in the fraction containing the washed LsrR protein (Figure 3, lane 3). As a control, we carried out the same series of experiments with bovine serum albumin (BSA) substituted for the LsrR protein (Figure 3, lanes 4–6). Both products X and Y are found in the filtrate following incubation with BSA (Figure 3, lane 5); however, neither product remains in the protein fraction (Figure 3, lane 6). These results demonstrate that the product X formed from reaction of LsrK with DPD is specifically bound by LsrR. This result

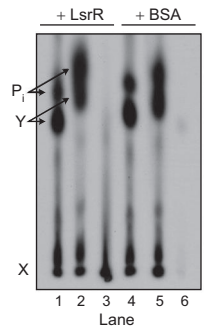

Figure 3. LsrR binds the phosphorylated product of the LsrK reaction. LsrK was incubated with synthetically prepared DPD and [γ-^{32}P]ATP for 120 min to allow the formation of products X and Y. Subsequently, this reaction mixture was incubated with LsrR protein (lanes 1–3) or with BSA (lanes 4–6) for 10 min at 37 °C. Aliquots from the LsrR and BSA incubations were spotted onto the TLC plate (lanes 1 and 4, respectively). The reaction mixtures were filtered to remove protein, and the protein-free fractions were applied to lanes 2 and 5. The protein-containing fractions were washed three times, and spotted in lanes 3 and 6. Filtration and washing steps were performed at 4 °C. Note that P_i and the product Y migrate slightly differently depending on the presence or the absence of proteins (LsrR or BSA), and this is indicated by the arrows.

TABLE 1. Products of the LsrK and LsrG catalyzed reactions

Reactions	Substrates	Enzymes	Mass Spectrometry[a] (ion counts × 10^3)				
			DPD	ATP	ADP	P-DPD	PG
1	ATP	LsrK	–[b]	110	12	–[b]	[c]
2	DPD	LsrK	110	–[b]	–[b]	–[b]	[c]
3	ATP + DPD		130	79	9	–[b]	–[b]
4	ATP + DPD	LsrK	15	6	120	57	–[b]
5	ATP + DPD	LsrG	52	25	4	–[b]	–[b]
6	ATP + DPD	LsrK + LsrG	3	3	65	0.8	24

[a]Reactions were incubated for 15 min at 37 °C. Subsequently, the reaction mixtures were analyzed by LC-MS/MS. The following compounds were detected: DPD (selected reaction monitoring (SRM) *m/z* 131 → 101 at 10 eV); ATP (SRM *m/z* 506 → 408 at 21 eV); ADP (SRM *m/z* 426 → 134 at 24 eV); DPD-P (SRM *m/z* 211 → 79 at 20 eV); PG (SRM *m/z* 155 → 79 at 20 eV). [b]Below the limit of detection. [c]Not determined.

strongly supports the idea that product X, which again we claim is P-DPD, is the critical one in *lsr* regulation.

LsrK Phosphorylates the Open Form of DPD at the C5 Position. MS analysis reveals that incubation of DPD and ATP with purified LsrK protein results in formation of a product of *m/z* 211 in negative ion mode (Table 1, reaction 4). This product was identified by MS/MS scanning for phosphorylated species, that is, parent ions that release fragments of *m/z* 79 (PO_3^-) or 97 ($H_2PO_4^-$) in MS/MS. The production of these daughter ions from *m/z* 211 strongly suggests that the parent molecule contains one phosphate group (sulfate is another possibility based on mass, but no sulfate was present in the reaction mixture). This product is consistent with addition of a phosphate group to DPD (MW(P-DPD) = 212). Formation of this phosphorylated product was not observed in reaction mixtures lacking the enzyme or any one of the substrates (Table 1, reactions 1–3). Furthermore, in reaction mixtures containing all three components (LsrK, DPD, ATP), DPD and ATP were substantially reduced and ADP was formed (Table 1, reaction 4), as determined by MS/MS analysis using selected reaction monitoring scans specific for the analytes of interest (*14*). Based on the MS data, we suggest that the product of LsrK action on DPD is a monophosphorylated derivative of DPD (P-DPD).

Validation for the formation of P-DPD and identification of the site of phosphorylation on DPD came from NMR studies. As we reported previously, in solution, DPD rearranges and exists as an equilibrium mixture composed of three predominant forms, one open form and two cyclic forms (Figure 1, panel a (*15, 16*)), as shown in the most relevant segment of the ^{1}H NMR spectrum of DPD (Figure 4, upper-left trace). As expected, there is no signal in the ^{31}P spectrum of this sample (Figure 4, upper-right trace). The gradually increasing baseline in this trace is a shoulder due to the large phosphate peak of the buffer. Addition of LsrK enzyme and ATP to DPD causes new ^{1}H multiplets to appear, which are denoted by the three connected vertical lines (Figure 4, middle-left trace). A single ^{31}P resonance arises at 4.21 ppm (middle-right trace) and is consistent with the formation of P-DPD. Importantly, this resonance appears as a triplet in the ^{31}P-NMR spectrum when proton coupling is allowed (Figure 4, insert above the middle right trace), which is in accord with the three-bond phosphorous coupling to a pair of CH_2 protons and the flexible open-chain structure. This pattern is consistent only with phosphorylation of the open-chain form of DPD at the C5 position and must occur from coupling of phosphorous with the two protons of the C5-CH_2 moiety. If one of the cyclic forms (Figure 1, panel a) was phosphorylated, this three-bond coupling to a pair of CH_2 protons could not be observed. For example, phosphorylation at the C4 position of either the open or the cyclic forms would produce only a doublet in the ^{31}P-NMR spectrum from phosphorous–proton coupling of the proton on the C4-CH group and can therefore be eliminated as a possibility.

Using ^{1}H NMR, we demonstrated that the ^{1}H multiplets that appear following incubation of LsrK with DPD and ATP are consistent with DPD phosphorylated at the C5 site. Specifically, we monitored the changes occurring in the ^{1}H-multiplet pattern after ^{31}P selective irradiation was applied at 4.21 ppm. (This is the frequency corresponding to the phosphorous resonance detected

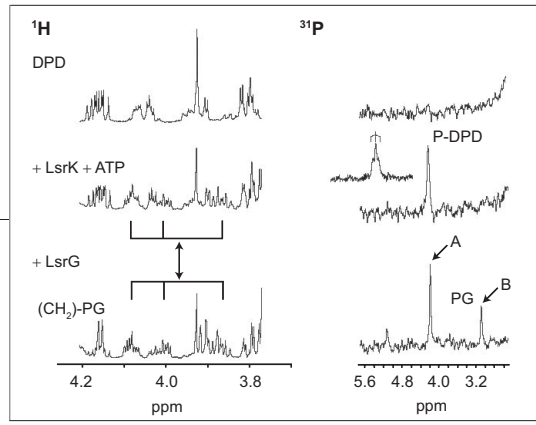

Figure 4. ^{1}H and ^{31}P NMR analysis of DPD and its derivatives. Most relevant segments of the ^{1}H spectra (left column) and the ^{31}P spectra (right column) are shown. The upper traces show DPD alone and that it has no associated phosphorus. The center traces result from incubating DPD with ATP and LsrK. The bottom traces show the status of the sample when LsrG is also added to the mixture. Addition of LsrK causes a new pattern in the ^{1}H spectra for the CH(OH)—CH$_2$—O-moiety of DPD. Vertical bars denote the positions of these protons at 4.07 ppm, 3.99 ppm, and 3.85 ppm, respectively. The resonance at 4.21 in the phosphorous spectra (middle-right trace) was assigned to the phosphate group of DPD (marked as P-DPD). The insert shows the phosphate spectrum of this group when proton-coupling is allowed. Addition of LsrG (bottom traces) results in a new doublet at 4.16 ppm in the proton spectra, which we assigned to the CH$_2$ protons from PG (highlighted as (CH$_2$)-PG)), and a singlet in the phosphorous spectra at 3.08 ppm, which we assigned to the phosphate group of the same product (highlighted as PG). Selective ^{31}P irradiation positions are indicated (A and B sites, respectively). The spectra of the samples taken following LsrG reaction reveal that some P-DPD remains (resonance at 4.21, bottom-right trace). Thus, not all the P-DPD is converted to PG, which is consistent with the TLC and MS results. The LsrG phosphorous spectrum also shows that an additional minor product at 5.13 ppm is formed. We do not know the identity of this minor compound.

following incubation of DPD with LsrK (P-DPD; A site, Figure 4)). The proton spectrum (Figure 5, panel a, bottom trace) shows that two nonequivalent —C**H**$_2$— CH(OH) protons appear each with ddd multiplet structure. By contrast, the CH$_2$—C**H**(OH) proton resonates at 4.07 ppm with a simpler dd multiple structure. Upon selective ^{31}P decoupling (A site, see Figure 4), only the multiplets for the CH$_2$ protons simplify to a dd structure (Figure 5, panel a, middle trace). The exclusive change in the CH$_2$ multiplet structure due to ^{31}P coupling from P-DPD is highlighted in the difference spectrum (Figure 5, panel a, top trace). We note that no changes in resonances are observed in the CH proton region (4.07 ppm, Figure 5, panel a, top trace) showing that ^{31}P decoupling does not affect the proton from the CH group. The measured coupling constants are as follows: $\delta = 4.07$ ppm, dd, $^3J_{H,H} = 6.8$ Hz, $^3J_{H,H} = 3.6$ Hz; $\delta = 3.99$ ppm, ddd, $^2J_{H,H} = 11.3$ Hz, $^3J_{H,H} = 3.6$ Hz, $^3J_{H,P} = 6.7$ Hz; and $\delta = 3.85$ ppm, ddd, $^2J_{H,H} = 11.3$ Hz, $^3J_{H,H} = 6.8$ Hz, $^3J_{H,P} = 6.7$ Hz. Further evidence for the assignment of P-DPD is provided in Supporting Information. The NMR results and the molecular weight data from MS are fully consistent with assignment of phosphorylation of DPD at C5 (P—O—CH$_2$—HCOH—CO—CO—CH$_3$) and establish that the final product of LsrK reaction is C5 phosphorylated DPD (Figure 6).

Analysis of the Products of the LsrG Reaction. Our previous genetic analyses suggested that LsrG is involved in processing the product of the LsrK reaction (*13*), which here we identify as P-DPD (Figure 6). Database analysis shows that LsrG has homology to several proteins in different bacteria; however, in every case, their functions are unknown. To test whether it plays a role in P-DPD metabolism, we purified the LsrG protein and incubated it with DPD and [γ-^{32}P]ATP both in the presence and in the absence of LsrK protein. No change in reactants occurred in the absence of LsrK as judged by TLC analysis (data not shown). However, incubation of LsrG with DPD, [γ-^{32}P]ATP, and LsrK (Figure 7, panel a) results in the immediate formation of the Y product (following the nomenclature introduced above for the TLC

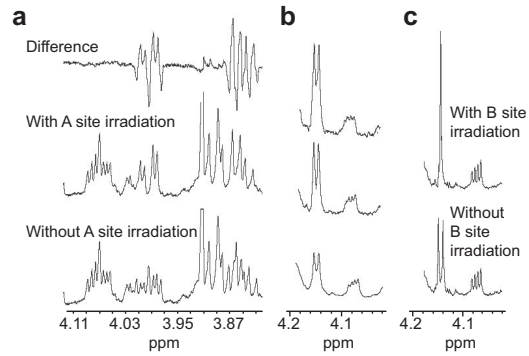

Figure 5. NMR identification of P-DPD and PG. a) Decoupling difference results following selective irradiation of the ^{31}P signal at 4.21 ppm (A site in Figure 4). Proton spectra of the products of the LsrK reaction without (bottom trace) or with (center trace) selective irradiation and the difference in the two spectra (upper trace). b) Results following spiking of the final reaction mixture containing DPD, ATP, LsrK, and LsrG with commercially obtained PG in two consecutive steps (middle and top traces, respectively). Spiking leads to a gradual increase in the doublet at 4.16 ppm. c) Decoupling results from selective irradiation of the ^{31}P resonance at 3.08 ppm (B site in Figure 4). The collapsing doublet (upper trace) proves the coupling between the new proton resonance at 4.16 ppm and the phosphorous resonance at 3.08 ppm, which appear after addition of the LsrG protein to the reaction mixture.

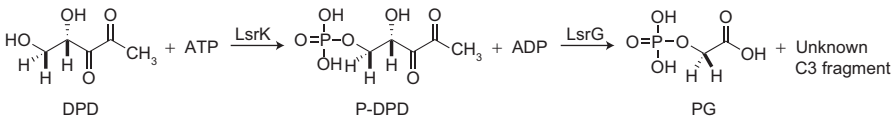

Figure 6. LsrK and LsrG processing of AI-2. In the presence of ATP, the LsrK kinase phosphorylates DPD at carbon-5 with the concomitant production of ADP. P-DPD is cleaved by LsrG to PG and an unidentified compound presumably containing three carbon atoms.

products, Figure 2). This result is strikingly different from what we observe following reaction with LsrK enzyme only (see Figure 2, panel b). In both experiments, the majority of the ATP is hydrolyzed after 10 min. In the incubation containing LsrK but no LsrG (Figure 2, panel b), X is the predominant product, and only trace amounts of the Y product are formed even after 60 min. By contrast, in the incubation containing both LsrK and LsrG(Figure 7, panel a), Y is the major product at 10 min. This led us to predict that LsrG catalyzes the conversion of product X (*e.g.*, P-DPD) to product Y. Consistent with this hypothesis, when we perform the LsrK and LsrG reactions sequentially, we observe nearly complete conversion of product X into product Y (Figure 7, panel b). Therefore, although product X (P-DPD) can spontaneously convert into product Y, this conversion is catalyzed by LsrG.

Mass spectral analysis shows that inclusion of the LsrG enzyme in reactions containing LsrK, DPD, and ATP results in consumption of DPD and ATP and formation of ADP and P-DPD (Table 1, reaction 6). However, much less P-DPD is detected when LsrG is present than in incubations containing only the LsrK enzyme (compare reactions 6 and 4). Presumably this is due to LsrG acting on the product (P-DPD) formed by LsrK, which would be consistent with the results obtained by TLC. To assay for possible products derived from P-DPD through the reaction catalyzed by LsrG, we again used MS to scan for phosphorylated species, that is, parent ions releasing MW 79 (PO_3^-) or 97 ($H_2PO_4^-$) fragments. We observed formation of a compound of m/z 155 only in reaction mixtures containing all the components (DPD, ATP, and both LsrK and LsrG, 15 min incubation time, Table 1, reaction 6). Again, consistent with the TLC studies showing the spontaneous conversion of P-DPD to the LsrG product (Figure 2), we found that the m/z 155 product could also be detected by MS in reaction mixtures that lacked LsrG but were incubated for very long times (4 h at 37 °C) with LsrK (data not shown).

Interestingly, one known phosphorylated compound of MW 156 (consistent with m/z 155 in negative ion mode) is reported in the Ecocyc database (www.ecocyc.org/): PG (Figure 6). To test whether PG is the product of reaction of LsrG with P-DPD, we compared the characteristics of authentic PG with the product present in our reaction mixtures using LC/tandem MS and NMR. The commercially obtained PG showed MS/MS fragmentation identical to the LsrG product. In addition, the chromatographic retention time (14.6 min using the hydrophilic interaction chromatography method (*14*)) of the LsrG product exactly matched that of PG.

The identification of PG as one product of the LsrG reaction with P-DPD was confirmed by NMR. Addition of LsrG to the reaction mixture containing DPD, LsrK, and ATP resulted in the appearance of a simple doublet resonance ($^3J_{H,P} = 5.5$ Hz) in the proton NMR spectrum at 4.16 ppm (denoted (CH_2)-PG in Figure 4, left bottom trace) and a new resonance at 3.08 ppm in the ^{31}P-spectrum (Figure 4, B site). Spiking of an LsrG reaction mixture with pure synthetic PG standard resulted in a perfect overlap of the doublet at 4.16 ppm and an increase in its intensity (Figure 5, panel b). Moreover, this resonance collapses to a singlet when ^{31}P selective irradiation was applied at 3.08 ppm (Figure 5, panel c), confirming that the resonance highlighted as site B (Figure 4) corresponds to the phosphorous group of PG. Our results are consistent with LsrG catalyzing the cleavage of P-DPD to PG and another three-carbon compound, which we are currently attempting to identify. LsrR does not bind the product of the LsrG reaction (Figure 3, Y). Therefore, we suggest that degradation of P-DPD by LsrG is the first step in terminating induction of the *lsr* operon.

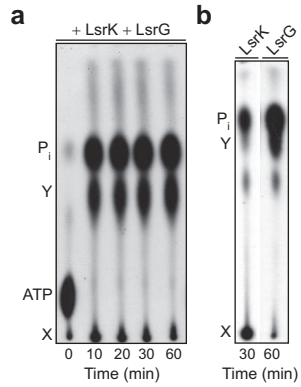

Figure 7. Analysis of LsrG reaction with P-DPD. TLC analysis with [γ-^{32}P]ATP, P$_i$, and the phosphorylated products X (P-DPD) and Y marked. a) LsrK and LsrG were simultaneously incubated with [γ-^{32}P]ATP and DPD. At the indicated times, aliquots of the reaction mixture were applied to the TLC plate. b) LsrK was incubated with [γ-^{32}P]ATP and DPD for 30 min to allow the formation of P-DPD (denoted X, left lane). LsrG was added, and the reaction continued for an additional 30 min followed by spotting onto the TLC plate (right lane).

Concluding Remarks. LsrB, the receptor for the AI-2 signal in enteric bacteria binds to (2*R*,4*S*)-2-methyl-2,3,3,4-tetrahydroxy-

tetrahydrofuran (*R*-THMF), a cyclic derivative of DPD that forms spontaneously in solution (Figure 1, panel A and ref *7*). Presumably, the LsrB-*R*-THMF complex interacts with the other components of the Lsr transporter to import this particular DPD derivative. Once in the cytoplasm, the molecule is phosphorylated by the LsrK kinase. LsrK phosphorylates the carbon atom in the 5-postition of the open form of DPD (Figure 6), showing that *R*-THMF must ring-open during the course of transport across the membrane, upon entering the cytoplasm, or upon binding by LsrK. We do not suspect that any other enzymes are involved in ring opening because we have shown previously that open and closed derivatives of DPD rapidly and spontaneously interconvert in solution (*7, 16*). A similar phenomenon occurs in ribose transport and phosphorylation. Ribose exists in different conformations in solution. In *E. coli,* the ribose-binding protein binds the β-D-pyranoribose form in the periplasm (*17*), while the ribokinase responsible for phosphorylation of ribose in the cytoplasm recognizes the α-D-ribofuranose form as substrate (*18*). We have also shown that the product of the LsrK reaction (P-DPD) is specifically bound by the repressor of the *lsr* operon, LsrR, supporting our genetic evidence that a phosphorylated form of the AI-2 signal is the inducer of the *lsr* operon as proposed (Figure 1, panel b).

To begin to define the subsequent events in AI-2 processing, we purified LsrG and showed that it cleaves P-DPD producing PG. Importantly, our results demonstrate that formation of PG from P-DPD can occur spontaneously, albeit at a very slow rate. Our previous genetic studies indicated that LsrG and LsrF are both involved in processing P-DPD (Figure 1, panel b). However, those initial studies did not provide information about which enzyme acted first on the product of the LsrK reaction. The present results show that, in fact, LsrG is the first enzyme to act. Additionally, our finding that the reaction catalyzed by LsrG can occur spontaneously explains our previous genetic analysis in which *lsrFG* double mutants could be partially complemented with either LsrF or LsrG (*13*). Indeed, our present findings suggest that the substrate for LsrF is likely present in *lsrG* mutant strains. We are characterizing the LsrF enzymatic activity to verify this hypothesis.

Currently, we do not understand the mechanism of the LsrG reaction. Considering that LsrG catalyzes the cleavage of P-DPD to PG, the most obvious second product would be hydroxyacetone, which could be obtained by a series of enolization, hydration, and retro-aldol reactions. Surprisingly however, we did not observe peaks that would correspond to hydroxyacetone in our NMR spectra. We also did not detect increases in existing NMR resonances when we spiked the LsrG reaction mixtures with authentic hydroxyacetone. Thus, the second product of LsrG reaction remains to be identified.

While we do not know the subsequent fate of the PG that is produced as a consequence of Lsr activity, it is known that, in bacteria, PG is produced during DNA repair and it is degraded to glycolate by a 2-phosphoglycolate phosphatase (*19*). In *E. coli*, the gene specifying the phosphatase (*gph*) is a member of the *dam* operon, the components of which function in surveillance of DNA fidelity. Interestingly, another gene in the *E. coli dam* operon is *rpe*, which is located upstream of *gph*. The *rpe* gene is homologous to *lsrE*, a gene encoded in several bacterial *lsr* operons, including those of *S. typhimurium*, *Yersinia pestis*, and *Pasteurella multocida* (*20*). The *lsrE* gene is not present in the *E. coli lsr* operon presumably because it is instead located in the *dam* operon.

We have previously demonstrated that enteric bacteria can use the Lsr transport system to interfere with AI-2-controlled behaviors of other species of bacteria in the vicinity. A molecular understanding of this and other natural strategies used by bacteria to interfere with one another's communication abilities can be viewed as models for the design of synthetic strategies aimed at manipulating bacterial behaviors. Such strategies show promise as new therapies for controlling quorum-sensing-regulated functions, such as virulence, and as biotechnological applications for enhancing industrial-scale production of beneficial bacterial products, such as recombinant proteins. Here we have studied the functions of the LsrK and LsrG proteins and showed that these two proteins are involved in the initial modification of the AI-2 signal molecule, and therefore, LsrK and LsrG play essential roles in the AI-2 interference mechanism.

MATERIALS AND METHODS

Overexpression and Purification of LsrK, LsrR, and LsrG. *S. typhimurium* LsrK with a C-terminal hexa-histidine tag was purified from *E. coli* strain BL21 containing the plasmid pMET1144 (*13*). The culture was grown at 37 °C to an OD_{600} of 0.3, transferred to 22 °C, and grown to an OD_{600} of 0.9. Expression was subsequently induced with 0.1 mM IPTG for 9 h. Cells were harvested and resuspended in 25 mM potassium phosphate, pH 7.1, 50 mM NaCl, 10 mM β-mercaptoethanol, 1 mM $MgCl_2$, 2.5 μg mL^{-1} DNase, and protease inhibitors (1 mM Pefablock, 2.5 μg mL^{-1} aprotinin, 2.5 μg mL^{-1} leupeptin). The cells were lysed with a Microfluidics M-110 Y microfluidizer and subjected to centrifugation to clear whole cells and cell debris. Supernatants were subjected to Ni–nitiloacetic acid chromatography with 50 mM potassium phosphate, pH 7.1, 10 mM imidazole, 20 mM β-mercaptoethanol, 50 mM NaCl, 1 mM $MgCl_2$ as the equilibration buffer. The same buffer containing 0.25 M imidazole was used to elute protein from the column. The protein was transferred to 25 mM potassium phosphate, pH 7.1, 1 mM DTT, 1 mM $MgCl_2$ *via* size-exclusion chromatography with G25 resin. The protein was concentrated to ~2 mg mL^{-1}, and 10% glycerol was added for stabilization purposes.

The *lsrR* gene from *S. typhimurium* and *lsrG* gene from *E. coli* were cloned into pGEX4T1 for expression as glutathione-S-transferase (GST) fusion proteins in *E. coli* strain BL21. The plasmids pMET1051 and pSTM1011 were used to express the GST-tagged LsrR and LsrG proteins, respectively, and were constructed with *lsrR* and *lsrG* DNA obtained by polymerase chain reaction amplification using the primers St36 (GCGGAATTCAGCCATAATACGTTGGTATCTG) and St37 (GCGCTCGAGTTCAATAATTTGAATTATTTTCCC) followed by digestion with *Eco*RI and *Xho*I for *lsrR* and primers EG5 (GAAGGATCCATGCACGTCACACT) and EG3 (GAACCCGGGTCACGGCATCAAA) followed by digestion with *Bam*HI and *Sma*I for *lsrG*.

N-terminal GST-tagged LsrR and LsrG were purified from *E. coli* strain BL21 containing the plasmids pMET1051 and pSM1011, respectively. Cultures were treated as above, but the resuspension buffer was 25 mM Tris, pH 8.0, 150 mM NaCl, 5 mM DTT, 2.5 μg mL^{-1} DNase, and protease inhibitors (1 mM Pefablock, 2.5 μg mL^{-1} aprotinin, 2.5 μg mL^{-1} leupeptin). Cells were lysed and centrifuged as previously described, and supernatants were purified by glutathione agarose chromatography with 25 mM Tris, pH 8.0, 150 mM NaCl, 1mM DTT as the equilibration buffer. The protein was eluted in 50 mM Tris, pH 8.0, 10 mM glutathione, 150 mM NaCl, and 1 mM DTT (or 5 mM in the case of LsrG) and concentrated to ~1 mg mL^{-1}. Purified LsrG was transferred to 25 mM potassium phosphate, pH 7.1, 1 mM DTT, 1 mM $MgCl_2$ *via* size-exclusion chromatography with G25 resin.

Chemical Methods. DPD protected with a cyclohexylidene group was chemically synthesized as reported previously (*16*). This compound was dissolved in water at concentrations of 10–25 mM. To remove the protecting group, the pH was lowered to below 2 for 4 h at RT followed by neutralization. For TLC and NMR analyses, 10 μL mL^{-1} of 1 M H_2SO_4 was used for deprotection and 1 M potassium phosphate buffer, pH 7.0, for neutralization. For MS analysis, 20 μL mL^{-1} of 1 M HCl was used for deprotection and 0.1 M NH_4OH for neutralization. PG, tri(monocyclohexylammonium) salt, was purchased from Akaal Organics.

TLC. LsrK, LsrG, or both (10 μg mL^{-1}) were incubated with 0.8 mM DPD, 20 mM phosphate buffer, pH 7.0, 60 μM ATP, 0.2 μCi of [γ-^{32}P]ATP, in 25 mM *N*-2-hydroxyethylpiperazine-*N*′-2-ethanesulfonic acid (HEPES) buffer, pH 7.5, with 0.240 mM $MgCl_2$ at 37 °C for various times, after which, 2 μL aliquots were applied to cellulose polyetherimide TLC plates (Scientific Absorbents). Plates were developed in 0.8 M LiCl, air-dried, and visualized by autoradiography. Proteins were removed by filtration at 4 °C with centrifuge filters, MWCO 5 kDa (UFV5BCC00, Millipore). Binding of P-DPD to LsrR was determined by mixing 10 μL of the LsrK reaction with 100 μL of LsrR (1 mg mL^{-1}), and 140 μL of 25 mM HEPES buffer, pH 7.5, with 0.240 mM $MgCl_2$. Following 10 min incubation at 37 °C, 20 μL of this mixture was applied to the TLC plate. The remainder of the sample was filtered as above. Subsequently, 20 μL of the protein-free fraction was applied to the TLC plate, and the protein-containing fraction was washed three times with 500 μL of 25 mM HEPES buffer, pH 7.5, with 0.240 mM $MgCl_2$. Following washing, the protein-containing fraction was resuspended in 100 μL of 25 mM HEPES buffer, pH 7.5, with 0.240 mM $MgCl_2$, and a 10 μL aliquot was applied to the TLC plate. The identical experiment was performed with BSA (Sigma).

NMR Analysis. ^{1}H NMR spectra were recorded on a Varian INOVA-600 instrument (Varian, Inc.) at 599.3 MHz at 4 °C in a D_2O/H_2O mixture using a PentaProbe (Varian, Inc.). For water suppression, excitation sculpting was applied (*21*). Chemical shifts were referenced to the water peak position (4.997 ppm at 4 °C). ^{31}P experiments were performed on a Varian INOVA-500 instrument at 202.3 MHz at 4 °C using broadband proton decoupling. Chemical shifts were referenced indirectly (through the lock signal) to 85% H_3PO_4/H_2O. LsrK and LsrG reactions were performed in 700 μL volumes containing combinations of the following components: 10 μg mL^{-1} protein, 6 mM DPD, 3 mM ATP, 12 mM $MgCl_2$, 60 mM potassium phosphate buffer, pH 7.0 (with 60% D_2O, Sigma). Reaction mixtures were incubated at 37 °C for 15 min. Reactions were terminated by placing on ice and were stored at 4 °C prior to NMR analysis.

MS. LsrK and LsrG reactions were performed in 100 μL reaction volumes containing combinations of the following components: 10 μg mL^{-1} of the indicated protein(s), 2.7 mM DPD (when indicated), and 1 mM ATP (when indicated) in 25 mM HEPES buffer, pH 7.5, with 4 mM $MgCl_2$. Note that DPD was prepared without H_2SO_4 and phosphate buffer because the presence of sulfate and phosphate in the reaction mixtures substantially complicates MS/MS detection of phosphorylated compounds. Reaction mixtures were incubated at 37 °C for 15 min. Reactions were terminated by placing onto ice (4 °C), and 90% methanol (in water) was added immediately thereafter to precipitate proteins and extract small molecules. The samples were allowed to stand for 10 min on ice, and precipitated proteins were removed by 5 min centrifugation at 4 °C (Eppendorf microcentrifuge, maximum speed) to yield a protein-depleted, small-molecule-enriched methanol extract appropriate for direct MS/MS analysis. MS analyses were performed on a Quantum Ultra triple-quadrupole mass spectrometer with electrospray ionization source (Thermo Electron Corp.). Compounds were detected in negative ionization mode with a spray voltage of 3000 V. Nitrogen was used as sheath gas at 30 psi and auxiliary gas at 10 psi, and argon was used as the collision gas at 1.5 mTorr, with the capillary temperature 325 °C.

For compounds where purified standards were available, MS/MS parameters (also commonly referred to as SRM parameters) could be determined by the instrument's automated fragmentation optimization routine, as described previously (*22*). By this method, DPD was determined to have a SRM of m/z 131 → 101 at 10 eV, ADP a SRM of m/z 426 → 134 at 24 eV, and ATP a SRM of 506 → 408 at 21 eV. Semiquantitative data shown in Table 1 were collected using these SRMs after sample injection using a LC-10A HPLC system (Shimadzu) with no chromatography column present (full quantitative analysis would have required use of chromatography, internal standards, or both to rule out minor ion suppression artifacts and was not conducted in a systematic fashion; however, preliminary experiments involving chromatographic separation confirmed all of the major trends shown in Table 1).

To search for possible reaction products for which standards were not available, a combination of parent scanning and product scanning in MS/MS mode was used. The most informative approach, given our anticipation based on the ^{32}P-labeling studies of phosphorylated reaction products, proved to be scanning for parent ions that yielded a product of *m/z* 79 (PO_3^-) or *m/z* 97 ($H_2PO_4^-$) upon MS/MS fragmentation (a variety of collision energies, from 10 to 60 eV, were tested to generate the fragments). This approach led to the identification of a prominent parent ion at *m/z* 211 in reaction 4 (Table 1) and *m/z* 155 in reaction 6 (Table 1), with no other major phosphorylated compounds detected (other than ADP and ATP). Subsequent product scans identified their optimal SRMs to be *m/z* 211 → 79 at 20 eV and *m/z* 155 → 79 at 20 eV, respectively. These SRMs were used to generate the data provided in Table 1.

To confirm that the compound with a parent mass of 155 was PG, we performed LC-MS/MS analysis involving hydrophilic interaction chromatography using an aminopropyl column at basic pH as described fully (*14*). We found a perfect retention time match between the commercial standard of PG and the product of reaction 6.

Acknowledgments: This work was funded by Howard Hughes Medical Institute, National Institutes of Health Grants GM 065859 and AI 054442, and National Science Foundation Grant MCB-0343821 (B.L.B.) and a Marie Curie International Reintegration Grant (European Commission, IRG-031108) (K.B.X.). We are grateful to Michiko Taga for plasmid pMET1051 and to members of Martin Semmelhack's laboratory for synthesizing DPD.

Supporting Information Available: This information is free of charge *via* the Internet.

REFERENCES

1. Waters, C. M., and Bassler, B. L. (2005) Quorum sensing: cell-to-cell communication in bacteria, *Annu. Rev. Cell Dev. Biol. 21*, 319–346.
2. Xavier, K. B., and Bassler, B. L. (2003) LuxS quorum sensing: more than just a numbers game, *Curr. Opin. Microbiol. 6*, 191–197.
3. Federle, M. J., and Bassler, B. L. (2003) Interspecies communication in bacteria, *J. Clin. Invest. 112*, 1291–1299.
4. Vendeville, A., Winzer, K., Heurlier, K., Tang, C. M., and Hardie, K. R. (2005) Making 'sense' of metabolism: autoinducer-2, LuxS and pathogenic bacteria, *Nat. Rev. Microbiol. 3*, 383–396.
5. Chen, X., Schauder, S., Potier, N., Van Dorsselaer, A., Pelczer, I., Bassler, B. L., and Hughson, F. M. (2002) Structural identification of a bacterial quorum-sensing signal containing boron, *Nature 415*, 545–549.
6. Miller, M. B., Skorupski, K., Lenz, D. H., Taylor, R. K., and Bassler, B. L. (2002) Parallel quorum sensing systems converge to regulate virulence in *Vibrio cholerae*, *Cell 110*, 303–314.
7. Miller, S. T., Xavier, K. B., Campagna, S. R., Taga, M. E., Semmelhack, M. F., Bassler, B. L., and Hughson, F. M. (2004) *Salmonella typhimurium* recognizes a chemically distinct form of the bacterial quorum-sensing signal AI-2, *Mol. Cell 15*, 677–687.
8. Taga, M. E., Semmelhack, J. L., and Bassler, B. L. (2001) The LuxS-dependent autoinducer AI-2 controls the expression of an ABC transporter that functions in AI-2 uptake in *Salmonella typhimurium*, *Mol. Microbiol. 42*, 777–793.
9. Xavier, K. B., and Bassler, B. L. (2005) Regulation of uptake and processing of the quorum-sensing autoinducer AI-2 in *Escherichia coli*, *J. Bacteriol. 187*, 238–248.
10. Schauder, S., Shokat, K., Surette, M. G., and Bassler, B. L. (2001) The LuxS family of bacterial autoinducers: biosynthesis of a novel quorum-sensing signal molecule, *Mol. Microbiol. 41*, 463–476.
11. Winzer, K., Hardie, K. R., Burgess, N., Doherty, N., Kirke, D., Holden, M. T., Linforth, R., Cornell, K. A., Taylor, A. J., Hill, P. J., and Williams, P. (2002) LuxS: its role in central metabolism and the *in vitro* synthesis of 4-hydroxy-5-methyl-3(2*H*)-furanone, *Microbiology 148*, 909–922.
12. Xavier, K. B., and Bassler, B. L. (2005) Interference with AI-2-mediated bacterial cell–cell communication, *Nature 437*, 750–753.
13. Taga, M. E., Miller, S. T., and Bassler, B. L. (2003) Lsr-mediated transport and processing of AI-2 in *Salmonella typhimurium*, *Mol. Microbiol. 50*, 1411–1427.
14. Bajad, S. U., Lu, W., Kimball, E. H., Yuan, J., Peterson, C., and Rabinowitz, J. D. (2006) Separation and quantitation of water soluble cellular metabolites by hydrophilic interaction chromatography-tandem mass spectrometry, *J. Chromatogr. A1125*, 76–88.
15. Meijler, M. M., Hom, L. G., Kaufmann, G. F., McKenzie, K. M., Sun, C., Moss, J. A., Matsushita, M., and Janda, K. D. (2004) Synthesis and biological validation of a ubiquitous quorum-sensing molecule, *Angew. Chem., Int. Ed. 43*, 2106–2108.
16. Semmelhack, M. F., Campagna, S. R., Federle, M. J., and Bassler, B. L. (2005) An expeditious synthesis of DPD and boron binding studies, *Org. Lett. 7*, 569–572.
17. Mowbray, S. L., and Cole, L. B. (1992) 1.7 Å X-ray structure of the periplasmic ribose receptor from *Escherichia coli*, *J. Mol. Biol. 225*, 155–175.
18. Sigrell, J. A., Cameron, A. D., Jones, T. A., and Mowbray, S. L. (1998) Structure of *Escherichia coli* ribokinase in complex with ribose and dinucleotide determined to 1.8 Å resolution: insights into a new family of kinase structures, *Structure 6*, 183–193.
19. Teresa Pellicer, M., Felisa Nunez, M., Aguilar, J., Badia, J., and Baldoma, L. (2003) Role of 2-phosphoglycolate phosphatase of *Escherichia coli* in metabolism of the 2-phosphoglycolate formed in DNA repair, *J. Bacteriol. 185*, 5815–5821.
20. Sun, J., Daniel, R., Wagner-Dobler, I., and Zeng, A. P. (2004) Is autoinducer-2 a universal signal for interspecies communication: a comparative genomic and phylogenetic analysis of the synthesis and signal transduction pathways, *BMC Evol. Biol. 4*, 36.
21. Hwang, T.-L., and Shaka, A. J. (1995) Water suppression that works. Excitation sculpting using arbitrary waveforms and pulsed field gradients, *J. Magn. Reson. A112*, 275–279.
22. Lu, W., Kimball, E., and Rabinowitz, J. D. (2006) A high-performance liquid chromatography–tandem mass spectrometry method for quantitation of nitrogen-containing intracellular metabolites, *J. Am. Soc. Mass Spectrom. 17*, 37–50.